ISET Journal of Earthquake Technology, Paper No. 494, Vol. 45, No. 1-2, March-June 2008, pp. 1–12

INFLUENCE OF LIQUEFACTION ON PILE-SOIL INTERACTION IN VERTICAL VIBRATION

B.K. Maheshwari*, U.K. Nath** and G. Ramasamy***

*Department of Earthquake Engineering, IIT Roorkee, Roorkee-247667
**Department of Civil Engineering, Jorhat Engineering College, Jorhat-285007
***Department of Civil Engineering, IIT Roorkee, Roorkee-247667

ABSTRACT

During strong earthquake shaking, loose cohesionless soils below the water table develop high pore water pressures and liquefy leading to significant degradation of strength and stiffness. In such soil stratum, pile foundations may undergo substantial shaking while the soil is in a fully liquefied state and soil stiffness is at its minimum. In this paper, an available numerical model formulating the pore pressure response directly from observed data on undrained tests has been used to study the liquefaction phenomenon. The Winkler soil model has been used to model the pile-soil interaction. Combining these two models, a formulation to predict the response of a pile in liquefiable soils in axial vibration is developed. It is observed that the response of a single pile due to axial vibration in liquefiable soil is significantly greater than that in non-liquefiable soil, particularly at higher frequencies.

KEYWORDS: Pile-Soil Interaction, Liquefaction, Winkler Soil Model, Numerical Models

INTRODUCTION

Damage to buildings, bridges, port facilities and other infrastructure during several major earthquakes has warranted attention of researchers towards the behavior of foundations under dynamic loading. Although studies of seismic loading of piles and of liquefaction phenomenon have been performed over the last four decades, the combined problem of seismic behavior of piles in liquefiable soil has received relatively less attention. Several experimental and analytical studies of this combined problem have been presented in the last five years (Finn and Fujita, 2002; Liyanapathirana and Poulos, 2005; Miwa et al., 2006). Yet much has to be revealed especially regarding the key aspects of influence of flow characteristic on this behavior. The excess pore pressure generated during liquefaction alters effective stresses in the soil and changes its mechanical behavior. The numerical formulation of the problem significantly reduces the computational effort needed for the solution.

During strong ground motion, piles are prone to severe cracking or even fracture. Liquefaction leads to substantial increase in the pile-cap displacements. After liquefaction, if the residual strength of the soil is less than the static shear stresses caused by a sloping site or a free surface such as a river-bank, significant lateral spreading or down-slope displacements may occur (Finn and Fujita, 2002). The moving soil can exert damaging pressures against the piles, leading to failure. Such failures were prevalent during the 1964 Niigata and the 1995 Kobe earthquakes. Seed and Idriss (1971), Martin and Seed (1979) observed the liquefaction phenomenon extensively and their model was based on the effective stress concept. Martin et al. (1975) showed that under drained conditions, loose sand would compact due to shearing.

Novak (1974) was first to use a Winkler model for the representation of a laterally loaded pile in a visco-elastic material. In Novak's solution, the soil is composed of horizontal layers that are homogenous, isotropic and linearly elastic. The soil reaction at any depth is that of an infinitely long rigid pile undergoing uniform harmonic vibration in an infinite medium and the plane strain conditions are assumed to hold. The pile foundations are subjected to axial vibration in many situations such as loading due to machinery and during earthquakes. Most of the initial reported research work on the soil-pile interaction was for vertical vibration. Nogami and Konagai (1986) and Konagai and Nogami (1987) suggested a simple mechanical model, which approximates the frequency-dependent behavior of plane-strain Winkler model used by Novak et al. (1978). El Naggar and Novak (1994) presented nonlinear soil model for axial pile response. Maheshwari et al. (2005) included the effects of soil plasticity while analyzing the soil-pile interaction.

The combined problem of pile-soil interaction and liquefaction has been studied only in the last decade. The measurements of dynamic *p-y* behavior for liquefying sand were presented by Wilson (1998), based on back-analyses of dynamic centrifuge model tests (Katsuichiro et al., 2004). Bhattacharya et al. (2004) reported buckling instability of pile foundations in liquefiable ground in axial direction. A pseudo-static approach has been adopted by Liyanapathirana and Poulos (2005), which involves two main steps. First, they carried out a nonlinear free-field site response analysis to obtain the maximum ground displacements along the pile and the degraded soil modulus over the depth of the soil deposit. In the second step, a static load analysis based on the maximum ground surface acceleration is performed.

The objective of this paper is to evaluate the response of a pile subjected to axial vibration in liquefiable soil taking into account the effects of pile-soil interaction. The analysis has been performed in the time domain. The degradation of the soil shear strength due to liquefaction is modeled using the numerical model proposed by Seed et al. (1976) and modified by Liyanapathirana and Poulos (2002a). Pile-soil interaction is incorporated in the model using the methodology suggested by Nogami and Konagai (1986) and extended by Konagai and Nogami (1987). Using this new methodology, the response of pile in liquefiable soils is predicted (Nath, 2006). Here, only a single end-bearing pile is considered. However, the model is capable of dealing with a pile group.

NUMERICAL FORMULATION

This is presented separately for liquefaction and for pile-soil interaction.

1. Modeling for Liquefaction

1.1 Zone of Liquefaction

It is important to check whether, for a given condition, the soil stratum liquefies. The first step in the analysis is to find the zone of liquefaction. This is determined by comparing the average shear stress τ_{av} due to earthquake loading and the shear stress τ causing liquefaction. The average shear stress is given by (Seed and Idriss, 1971)

$$\tau_{\text{av}} = 0.65 \frac{a_{\max}}{g} \sigma_v r_d \tag{1}$$

where, $a_{\max}$ is the peak ground acceleration, σ_v is the total overburden pressure, and r_d is the depth reduction factor. The shear stress causing liquefaction is given by (Prakash, 1981)

$$\left(\frac{\tau}{\sigma_v'} \right)_{D_r} = \left(\frac{\sigma_{dc}}{2\sigma_a} \right)_{50} C_r \frac{D_r}{50} \tag{2}$$

where, $(\sigma_{dc} / 2\sigma_a)_{50}$ is the cyclic stress ratio (CSR), which can be found from the charts (Seed and Idriss, 1971), provided D_{50} of the soil is known. The charts are prepared on the basis of a number of cyclic triaxial and simple shear tests. Separate charts are applicable for different numbers of cycles causing liquefaction, which, in turn, depend on the magnitude of the earthquake. Further, in Equation (2), D_r denotes the relative density of soil in percentage, and C_r is a correction factor, the value of which depends on D_r.

1.2 Numerical Model

The numerical modeling for the liquefaction of soil is based on Seed et al. (1976), and Liyanapathirana and Poulos (2002a). The three basic steps are evaluation of (a) rate of pore pressure generation, (b) pore pressure redistribution and dissipation, and (c) the stress response analysis with pore water pressure induced. These steps of numerical formulation are discussed in detail in Liyanapathirana and Poulos (2002a, 2002b), and are briefly described here.

Rate of Pore Pressure Generation, $\partial u_g / \partial t$: The rate of pore pressure generation during earthquake shaking is calculated as follows (Liyanapathirana and Poulos, 2002a):

$$\frac{\partial u_g}{\partial t} = \frac{\partial u_g}{\partial N}\frac{\partial N}{\partial t} = \frac{\sigma_{v0}^{/}}{\theta\pi N_L \sin^{2\theta-1}(\pi r_p/2)\cos(\pi r_p/2)}\frac{\partial N}{\partial t} \tag{3a}$$

where, u_g is the excess pore pressure generated due to earthquake loading; $\partial N/\partial t$ is the rate of application of shear stress cycles to the soil; $\sigma_{v0}^{/}$ is the initial effective overburden pressure; and r_p is the pore pressure ratio, i.e., the ratio of excess pore water pressure to initial effective overburden pressure. The shear stress rate $\partial N/\partial t$ can be worked out by first representing the actual stress time-history into an equivalent number N_{eq} of uniform stress cycles (Seed et al., 1976). For harmonic excitation, $\partial N/\partial t$ is simply the frequency of excitation. The value of r_p is given by the following expression:

$$r_p = \frac{u_g}{\sigma_{v0}^{/}} = \frac{2}{\pi}\sin^{-1}\left(\frac{N}{N_L}\right)^{\frac{1}{2\theta}} \tag{3b}$$

where, N_L is the number of uniform stress cycles required to produce a condition of initial liquefaction (i.e., excess pore pressure = effective confining pressure) under undrained conditions. The value of N_L can be read off from a family of curves (which are developed based on simple shear tests) as discussed by Seed et al. (1976). Further, N is the number of equivalent uniform cycles, for harmonic excitation $N = N_{\text{eq}}$, and can be worked with the magnitude of earthquake. The parameter θ is assumed as 0.7 in the analysis for the best fit.

Pore Pressure Redistribution and Dissipation: Considering pore pressure distribution within the soil due to vertical drainage, the net excess pore pressure $\partial u/\partial t$ developed in the soil, in one-dimensional formulation, is given by (Liyanapathirana and Poulos, 2002a)

$$\frac{\partial u}{\partial t} = \frac{1}{m_v\gamma_w}\frac{\partial}{\partial z}\left(k\frac{\partial u}{\partial z}\right) + \frac{\partial u_g}{\partial t} \tag{3c}$$

where, k is the permeability of the soil, m_v is the tangent coefficient of volume compressibility, γ_w is the unit weight of water, and $\partial u/\partial z$ is the gradient of excess pore pressure in the vertical direction. The value of m_v is given by the following expression:

$$\frac{m_v}{m_{v0}} = \frac{e^{ar_p^b}}{1 + ar_p^b + 0.5a^2 r_p^{2b}} \tag{3d}$$

where, m_{v0} is the tangent coefficient of volume compressibility at low pressure. The values of a and b are dependent on relative density of soil D_r and can be expressed as follows:

$$a = 5(1.5 - D_r) \text{ and } b = (3/2)^{2D_r} \tag{3e}$$

The value of m_{v0} may be taken as 26.1×10^{-6} m^2/kN and 41.8×10^{-6} m^2/kN for dense and loose soil, respectively (Seed et al., 1976).

Effective Stress Response Analysis with Pore Water Pressure Induced: Using Equation (3a) (for $N_{\text{eq}} < N_L$) generated pore water pressure, or using Equation (3c) (for $N_{\text{eq}} > N_L$ with $r_p = 1$), redistributed pore water pressure is determined. Thus the excess pressure, and in turn the effective stress, can be worked out. At the end of each loading and reloading phase, the soil stiffness is degraded based on the effective stress in the soil as (Liyanapathirana and Poulos, 2002a)

$$\frac{G_t}{G_0} = \left(\frac{\sigma'_{vt}}{\sigma'_{v0}}\right)^{\eta} \tag{3f}$$

Here G_t, G_0, σ'_{vt} and σ'_{v0} are the shear modulus at time t, the initial shear modulus, the effective overburden stress at time *t*, and the initial effective overburden stress, respectively. Further, η is the

power exponent and is generally equal to 0.5. The shear strength of the soil is also modified progressively as

$$\frac{\tau_{ft}}{\tau_{f0}} = \left(\frac{\sigma'_{vt}}{\sigma'_{v0}} \right)^{\eta} \tag{3g}$$

2. Modeling for Pile-Soil Interaction

First, configuration of the soil-pile system is discussed, followed by numerical modeling.

2.1 Configuration of the System

The configuration of the soil-pile system is shown in Figure 1. It is assumed that there is a hard stratum either at the pile tip or at some depth below the tip, so that piles which are not directly resting on the bedrock can be analyzed using the same methodology as the end-bearing piles by assuming a fictitious pile, made of soil below the pile tip. The pile-soil system is divided into horizontal slices containing the pile segment and homogenous soil layer. The Winkler soil model units are assumed to be uniformly distributed along the pile shaft for modeling the soil medium around the pile.

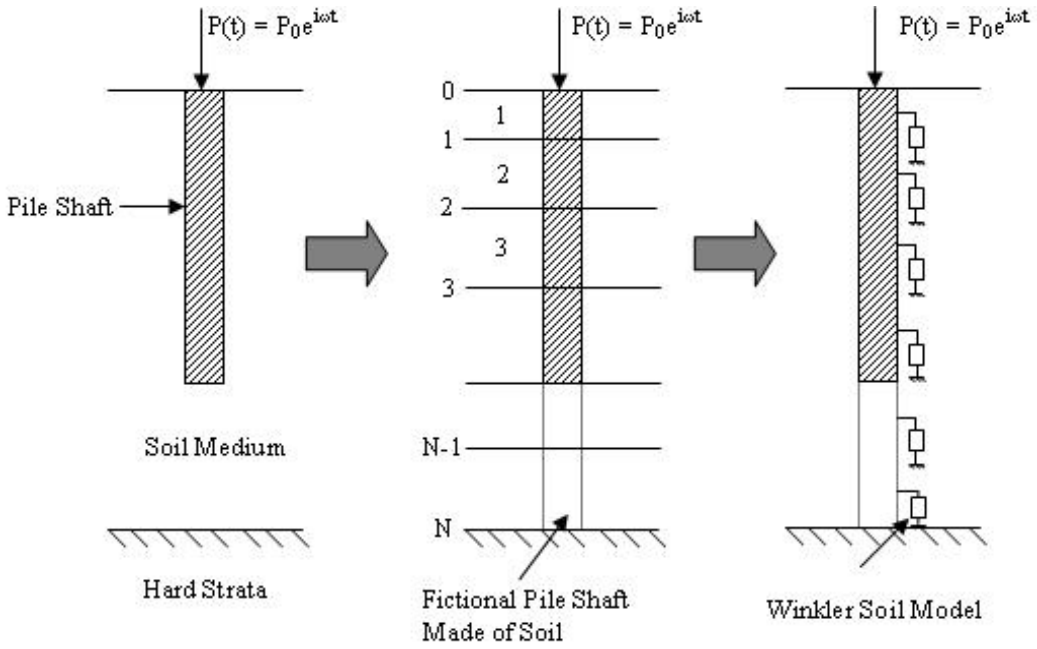

Fig. 1 Soil-pile system divided into horizontal slices

One unit of model is shown in Figure 2; this is shown in horizontal direction for convenience, although it is attached to the pile in the vertical direction.

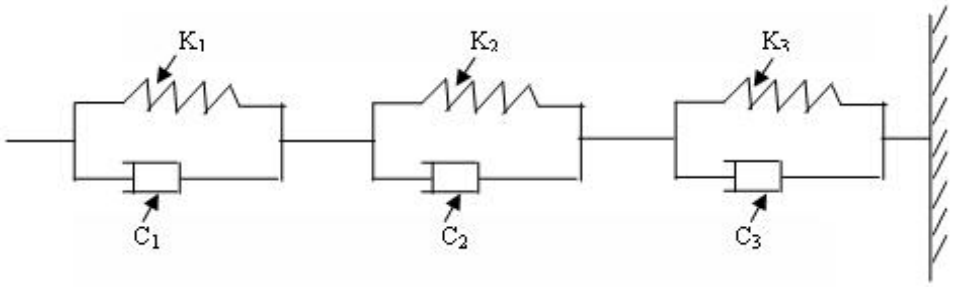

Fig. 2 One unit of Winkler soil model for the axial pile shaft response (shown in the horizontal direction for convenience; this is actually attached to the pile in the vertical direction)

For the axial loading, the values of the model parameters are determined using the following expressions (Nogami and Konagai, 1986):

$$\left(k_1, k_2, k_3\right) = G_s(3.518, 3.581, 5.529) \tag{4a}$$

$$\left(c_1, c_2, c_3\right) = \frac{G_s r_0}{V_s}(113.097, 25.133, 9.362) \tag{4b}$$

Here G_s, r_o, and V_s are shear modulus, radius of embedded pile, and shear wave velocity of the soil, respectively. It may be noted that these parameters are frequency-independent.

2.2 Numerical Modeling

The numerical model for vertical vibration (Nogami and Konagai, 1986) is based on Winkler's hypothesis, i.e., the soil-pile interaction force is related to the pile-shaft displacements only at that depth where the interaction force is considered. The pile-soil system is divided into number of layers (see Figure 1). Applying the boundary conditions at the two adjacent segments, the displacements and forces at the bottom of the *n*th segment of the pile shaft or soil column can be calculated as (Nogami and Konagai, 1986)

$$\begin{Bmatrix} w_i \\ P_i \end{Bmatrix}_n = \left[T_n\right] \begin{Bmatrix} w_i \\ P_i \end{Bmatrix}_0 + \left\{Q_n\right\} \tag{4c}$$

where,

$$\left[T_1\right] = \left[t_1\right] \text{ and } \left\{Q_1\right\} = \left[q_1\right]\left\{\gamma_{i,1}\right\} \text{ for } n = 1 \tag{4d}$$

and

$$\left[T_n\right] = \left[t_n\right]\left[T_{n-1}\right] \text{ and } \left\{Q_n\right\} = \left[t_n\right]\left\{Q_{n-1}\right\} + \left[q_n\right]\left\{\gamma_{i,n}\right\} \text{ for } n \geq 2 \tag{4e}$$

Here w_i and P_i are the axial pile displacement and applied axial load, respectively, and *n* indicates the number of layer. Also $[t]$ and $[q]$ are 2×2 matrices which are dependent on the material and geometrical properties of the pile, while γ_i is a vector. Details of these matrices and vector can be found in Nogami and Konagai (1986). The values of G_s are considered as G_0 and G_t (as obtained from Equation (3f)) for the analysis of pile-soil interaction in non-liquefiable soil and liquefiable soil, respectively.

Equations (4a)–(4e) are for a single pile; Konagai and Nogami (1987) extended this methodology for a pile group where displacement in soil at distance *r* from the source of disturbance (i.e., the pile axis) can be found. Thus shear strain, and in turn shear stress, developed in the soil medium due to vertical vibration can be estimated. Here it should be noted that soil is modeled using Winkler soil model which treats soil as a visco-elastic material, and that parameters are given by Equations (4a) and (4b). Further, no plasticity or yielding of soil is considered, though degradation of the material is taken into account using Equation (3f), which is based on the effective stress principle. An advanced plasticity-based model could also be considered.

VERIFICATION OF THE MODELS

Since a rigorous approach has been chosen for the soil-pile interaction and liquefaction analysis, verification of the models and computation technique is imperative. This is performed by comparing the results obtained from the present analysis with well-established results in literature. It may be noted that no commercial software has been used for the computations, and that a computer code has been developed in C++ language to compute the results presented here.

1. Verification for Complex Soil Stiffness

Modeling of the pile-soil interaction for axial load has been carried out using Winkler's hypothesis. A concrete pile of diameter 1 m, length 20 m, and fixed at the pile tip is considered. Figure 3 shows variation in dimensionless complex soil stiffness with dimensionless frequency a_0 $(= \omega r_0 / V_s)$ due to the application of axial load. It can be observed that the real part remains relatively constant with frequency while the imaginary part is linearly increasing. These trends of results are in very good agreement with

those presented by Nogami and Konagai (1986) and shown in Figure 3. This verifies the computational algorithm developed.

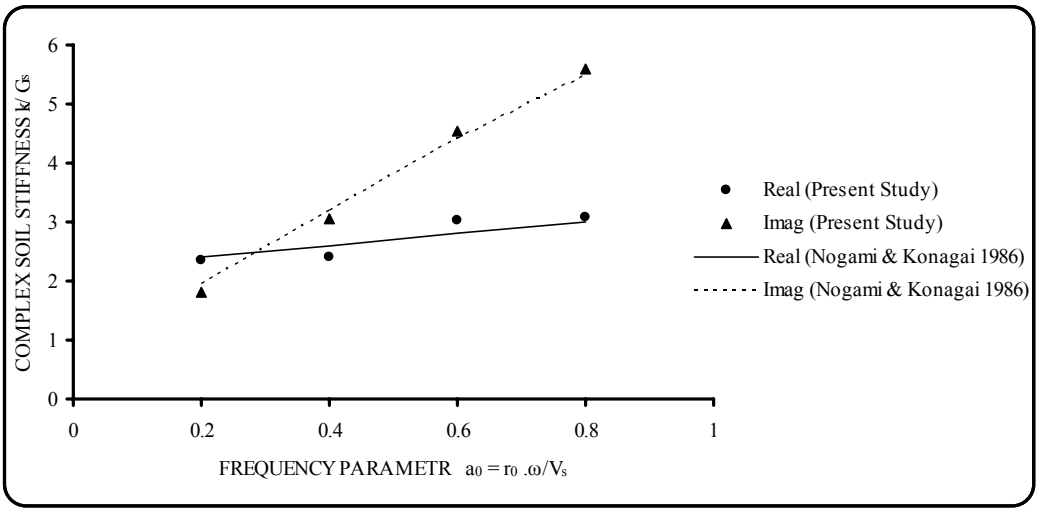

Fig. 3 Complex soil stiffness versus frequency: comparison of present study with Nogami and Konagai (1986)

2. Verification for Pile-Head Stiffness

Figure 4 shows the relationship between the dimensionless pile-head stiffness and dimensionless frequency due to the application of axial load. In this case also, trends of results are similar to those presented by Nogami and Konagai (1986). However, the imaginary part of the pile-head stiffness shown by the present study is significantly greater than that presented by Nogami and Konagai (1986), which may be attributed to the fact that slenderness ratio of the pile is different in the two cases.

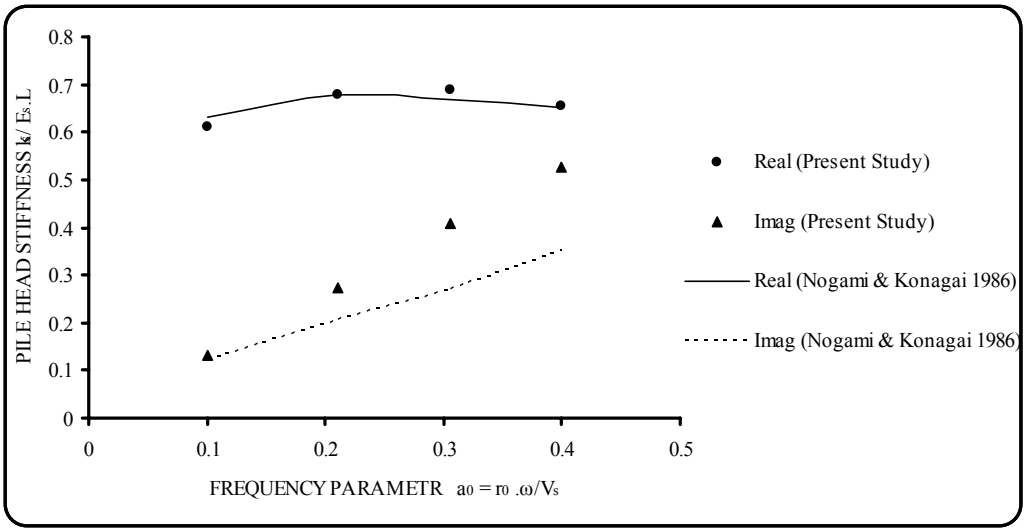

Fig. 4 Pile-head stiffness versus frequency: comparison of present study with Nogami and Konagai (1986)

3. Verification for Liquefaction Model

The result obtained from the liquefaction model is shown in Figure 5. It can be seen that the rate of generation of pore pressure first increases drastically and then decreases exponentially with number of cycles. Similar trend of results was shown by Gupta (1979).

DATA USED IN ANALYSIS

For the given soil profile, it is evaluated whether liquefaction will occur or not. First the zone of liquefaction is determined; for this purpose, the input data used in the analysis is shown in Table 1. A homogeneous soil stratum of 20 m depth is considered to be resting on the bedrock.

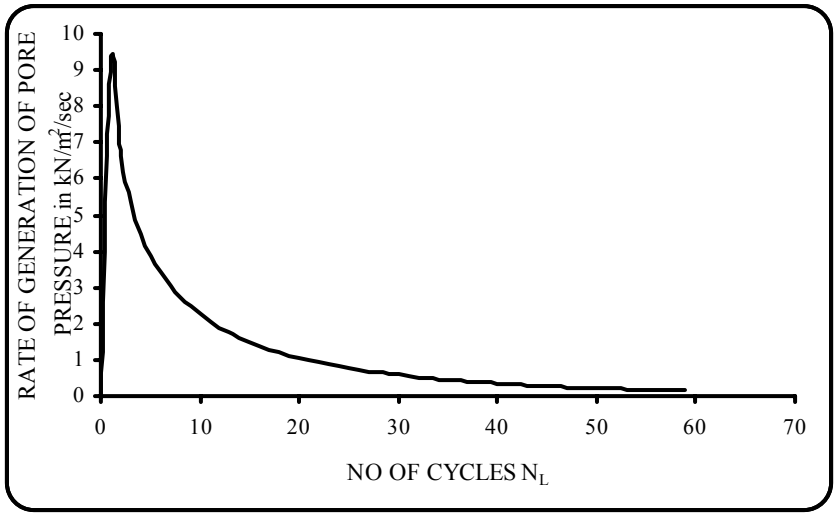

Fig. 5 Rate of generation of pore pressure versus number of cycles

Table 1: Input Data Used to Find the Zone of Liquefaction

Input Data	Value
PGA (a_{max})	0.16*g*
Magnitude of the earthquake (*M*)	7.5
Equivalent Number of Cycles (N_{eq}) for $M = 7.5$	20
D_{50} of sand	0.2 mm
Relative density (D_r)	40%
Thickness of soil stratum	20.0 m
Saturated mass density of soil (ρ_{sat})	1.804×10^3 kg/m^3

Zone of Liquefaction: Figure 6 shows a comparison of two sets of results, i.e., average shear stress τ_{av} versus depth (using Equation (1)) and shear stress causing liquefaction, τ , versus depth (using Equation (2)). It can be observed that for PGA equal to 0.16*g* and for earthquake of magnitude 7.5, soil stratum will liquefy for the whole depth. Here the position of water table is assumed at the ground surface itself. At higher depths, there is a wide margin between the two curves (see Figure 6), which may be attributed to the fact that relative density of the soil stratum is only 40% (for loose soil) and, therefore, it will be subjected to severe liquefaction.

RESULTS AND DISCUSSION

The behavior of soil-pile interaction is investigated in the following sections with respect to the variations in frequency of excitation and pile diameter. Effects of these parameters on the maximum displacement and interacting forces are evaluated considering liquefaction.

For the parametric study, the data used is shown in Table 2.

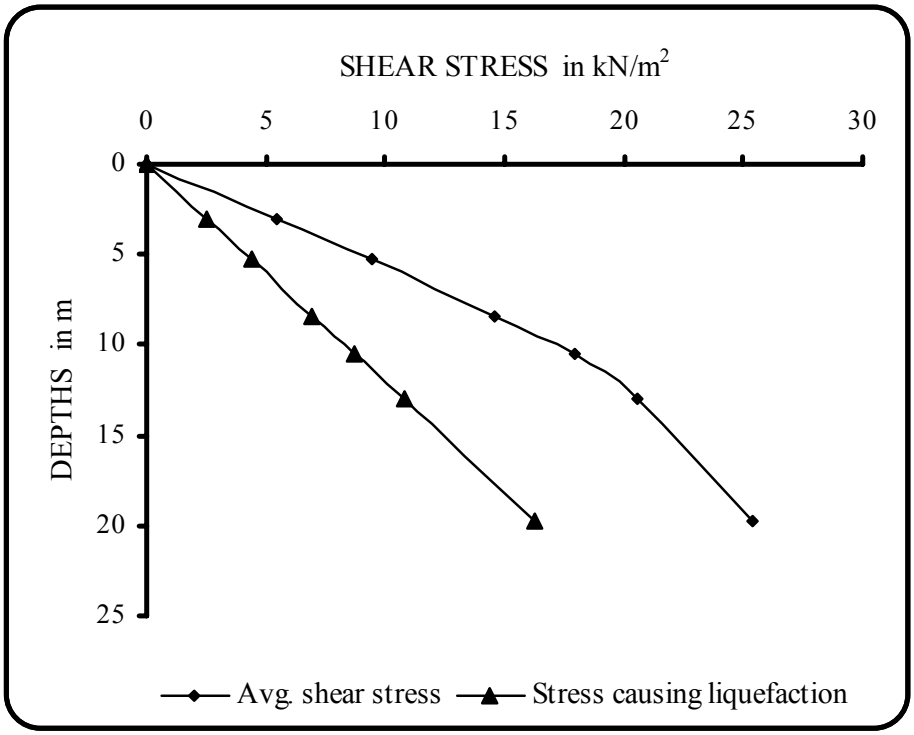

Fig. 6 Zone of liquefaction

Table 2: Input Data Used in the Parametric Study

Input Data	Value
Amplitude of harmonic force excitation (P)	100 kN
Dimensionless frequency of excitation (a_0)	0.1, 0.2, 0.3, 0.4
Pile diameter $(2r_0)$	1.0 m
Length of the pile	20.0 m
Modulus of elasticity of the pile (E_p)	25.00×10^9 N/m^2
Shear modulus of the soil (G_s)	71.77×10^6 N/m^2
Shear wave velocity (V_s)	199.46 m/s
Poisson's ratio of the soil (ν)	0.40

1. Effects of Frequency

Axial displacements due to the pile-soil interaction for different values of dimensionless frequency a_0 without and with liquefaction are compared in Figures 7(a) and 7(b), respectively.

In Figures 7(a) and 7(b), it may be observed that displacements at lower frequencies are more than those at the higher frequencies. This is because the dimensionless fundamental natural frequency a_0 of the soil is very low and close to the lowest frequency considered (= 0.1), with a_0 calculated as follows: $a_0 = \omega r_0/V_s = 2\pi\times f_0\times r_0/V_s = 2\pi\times V_s\times r_0/V_s\times 4h = \pi\times r_0/2h \approx 0.04$. Also for all frequencies, the maximum displacement is observed at the ground surface, which may be attributed to higher interacting

forces near the pile head. Also the effect of frequencies is diminishing at the higher values of a_0. The overall trend of the results is similar for both non-liquefied and liquefied cases.

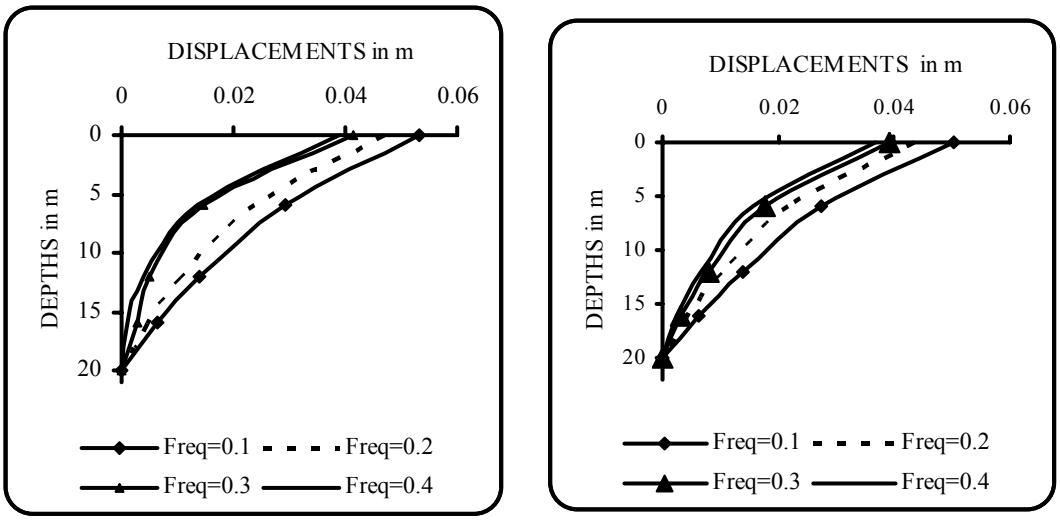

Fig. 7 Comparison of the axial displacements at different values of dimensionless frequency a_0 for the (a) non-liquefied and (b) liquefied cases

Interacting forces due to the pile-soil interaction (without and with liquefaction) for different frequencies are compared in Figures 8(a) and 8(b), respectively. The interacting forces increase with the frequency of excitation, when liquefaction is not considered. However, for the liquefied soil, the effect of frequency is not significant and peak value (at the ground surface) is lower than that in the non-liquefied case. Further, for the liquefied soil, it appears that the effect of liquefaction dominates over the frequency of excitation.

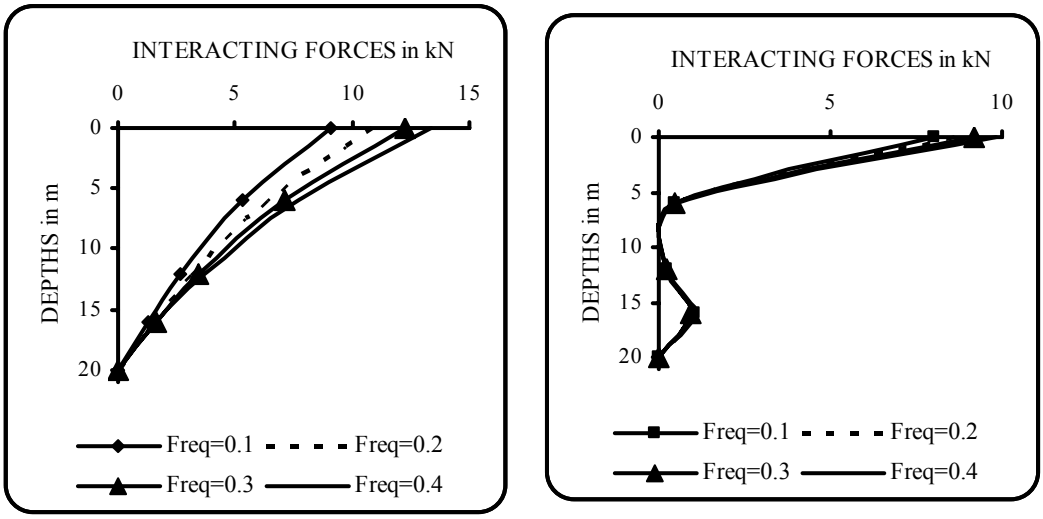

Fig. 8 Comparison of the interacting forces for different values of dimensionless frequency a_0 for the (a) non-liquefied and (b) liquefied cases

2. Effects of Liquefaction

Axial displacements for the non-liquefaction (NL) and liquefaction (L) conditions are compared in Figures 9(a) and 9(b) for the dimensionless frequencies equal to 0.3 and 0.4, respectively. The axial displacements at higher depths with liquefaction are greater than those without liquefaction. This is

because of the degradation of soil due to liquefaction. The percentage increase in the displacements due to liquefaction is observed as follows. For a_0 = 0.3, the percentage increase in the displacement is 22.76% and 36.3% at the depths of 6 and 12 m, respectively. Similarly for a_0 = 0.4, this increase is 12.9% and 42.6% at the depths of 6 and 12 m, respectively. Thus due to the effects of liquefaction, displacements are increased significantly.

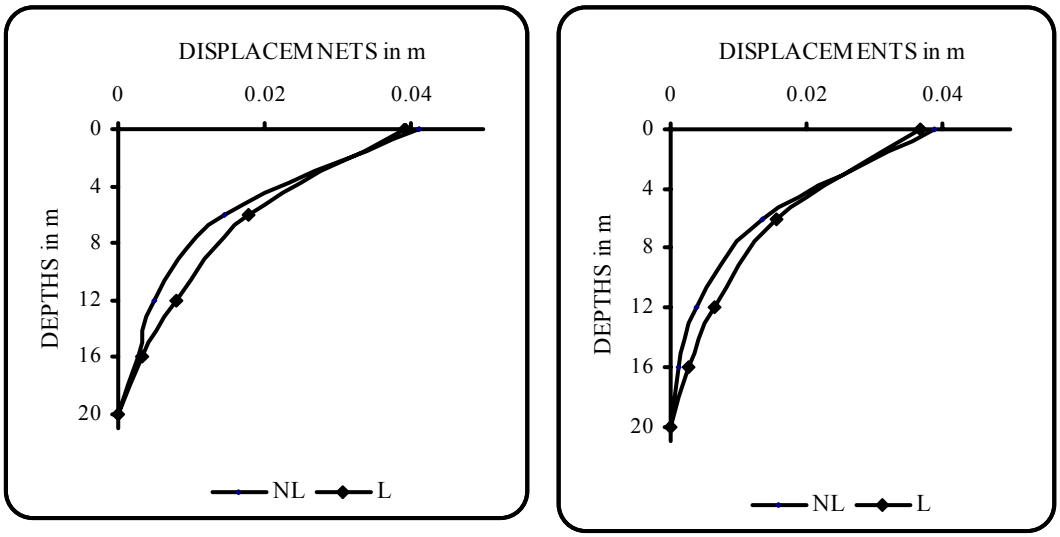

(a) (b)

Fig. 9 Effects of liquefaction on axial displacements for two different frequencies: (a) a_0 = 0.3, and (b) a_0 = 0.4

Figures 10(a) and 10(b) show the effects of liquefaction on the interacting forces for a_0 = 0.3 and 0.4, respectively. It can be observed that due to liquefaction, the interacting force is drastically reduced. It is because of the reduction in the shear strength of soil due to liquefaction that lower interacting forces are obtained.

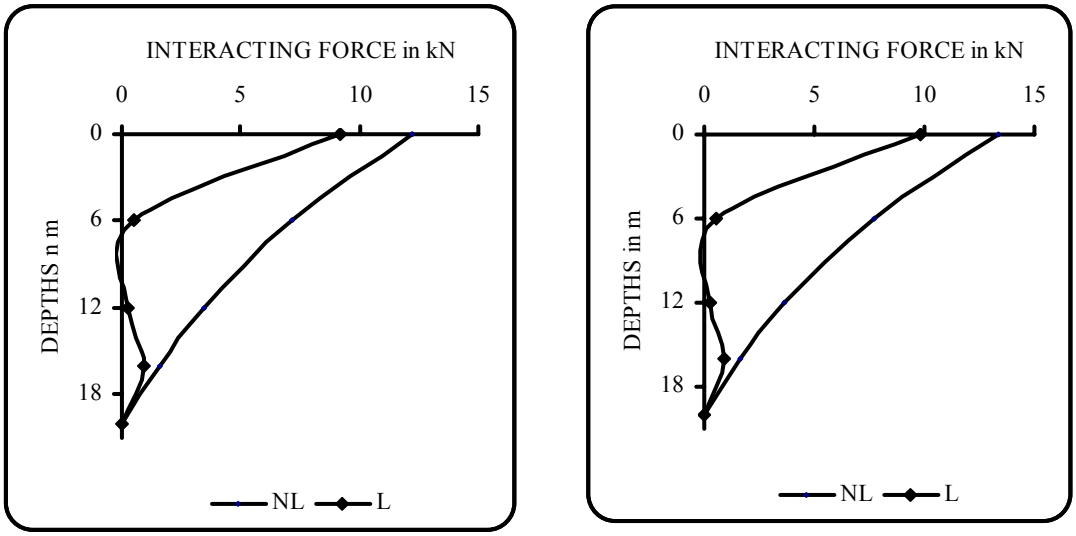

(a) (b)

Fig. 10 Effects of liquefaction on interacting forces for two different frequencies: (a) a_0 = 0.3, and (b) a_0 = 0.4

3. Effects of Pile Diameter

The effects of variation in geometric properties are considered by changing the diameter of the pile for the liquefiable soil. The diameters of the pile considered are d = 1 and 0.5 m. The results are shown in Figures 11(a) and 11(b) for a_0 = 0.3 and 0.4, respectively. For both frequencies, it can be observed that the displacements are considerably higher for the smaller diameter pile. This is as expected because decreasing the cross-sectional area would increase the stresses and thus the interaction forces; this, in turn, will increase the displacements. Thus a smaller diameter pile may be vulnerable to large displacements and also to instability failure in axial vibration (Bhattacharya et al., 2004).

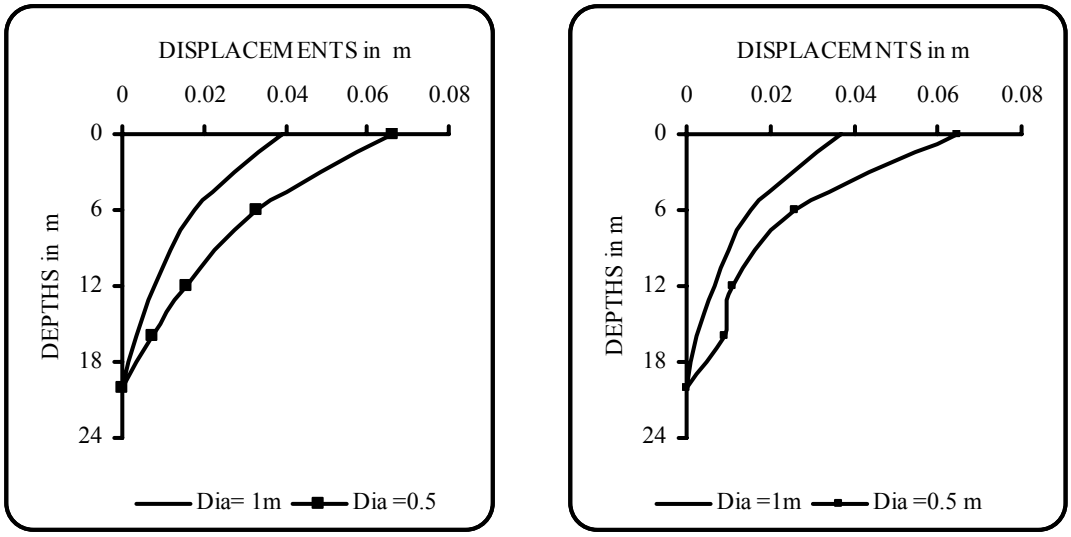

Fig. 11 Effects of pile diameter on axial displacements for two different frequencies (in liquefiable soil): (a) a_0 = 0.3, and (b) a_0 = 0.4

CONCLUSIONS

The following conclusions may be derived from this study:

1. The axial displacements developed due to the pile-soil interaction for different frequencies without and with liquefaction are significant near the natural frequency of the soil stratum.
2. Due to liquefaction, displacements are increased significantly while interaction forces decrease drastically.
3. Effect of frequency on both displacements and interaction forces is relatively small for liquefiable soils. It appears that the effect of liquefaction dominates over that of frequency.
4. In liquefiable soils, the displacements for small-diameter piles are considerably greater than those for the large-diameter piles.

In the present analysis, liquefaction has been considered along with the soil-pile interaction for axial vibration. This research work has wide practical applications in analyzing and designing pile foundations passing through liquefiable soil layers.

Here for simplicity, a simple visco-elastic soil model (i.e., Winkler soil model) has been considered in the analysis. However, the liquefaction being a nonlinear problem, an advanced constitutive model of soil with yielding of material may be considered. The results presented may differ in the case of the advanced soil model; nonetheless the paper demonstrates qualitatively the effects of liquefaction on soil-pile interaction in axial vibration.

REFERENCES

1. Bhattacharya, S., Madabhushi, S.P.G. and Bolton, M.D. (2004). “An Alternative Mechanism of Pile Failure in Liquefiable Deposits during Earthquakes”, Geotechnique, Vol. 54, No. 3, pp. 203–213.

2. El Naggar, M.H. and Novak, M. (1994). "Nonlinear Model for Dynamic Axial Pile Response", Journal of Geotechnical Engineering, ASCE, Vol. 120, No. 2, pp. 308–329.
3. Finn, W.D.L. and Fujita, N. (2002). "Piles in Liquefiable Soils: Seismic Analysis and Design Issues", Soil Dynamics and Earthquake Engineering, Vol. 22, No. 9–12, pp. 731–742.
4. Gupta, M.K. (1979). "Liquefaction of Sand during Earthquake", Ph.D. Dissertation, Department of Earthquake Engineering, University of Roorkee, Roorkee.
5. Katsuichiro, H., Tomoaki, I., Hideo, T., Kohji, K., Yuji, M., Osamu, K. and Robert, N. (2004). "Experimental Study on Soil-Pile-Structure Interaction in Liquefiable Sand Subjected to Blast-Induced Ground Motion", Proceedings of the 13th World Conference on Earthquake Engineering, Vancouver, Canada, Paper No. 190 (on CD).
6. Konagai, K. and Nogami, T. (1987). "Time Domain Axial Response of Dynamically Loaded Pile Groups", Journal of Engineering Mechanics, ASCE, Vol. 113, No. 3, pp. 417–430.
7. Liyanapathirana, D.S. and Poulos, H.G. (2002a). "Numerical Simulation of Soil Liquefaction due to Earthquake Loading", Soil Dynamics and Earthquake Engineering, Vol. 22, No. 7, pp. 511–523.
8. Liyanapathirana, D.S. and Poulos, H.G. (2002b). "A Numerical Model for Dynamic Soil Liquefaction Analysis", Soil Dynamics and Earthquake Engineering, Vol. 22, No. 9–12, pp. 1007–1015.
9. Liyanapathirana, D.S. and Poulos, H.G. (2005). "Pseudostatic Approach for Seismic Analysis of Piles in Liquefying Soil", Journal of Geotechnical and Geoenvironmental Engineering, ASCE, Vol. 131, No. 12, pp. 1480–1487.
10. Maheshwari, B.K., Truman, K.Z., Gould, P.L. and El Naggar, M.H. (2005). "Three-Dimensional Nonlinear Seismic Analysis of Single Piles Using Finite Element Model: Effects of Plasticity of Soil", International Journal of Geomechanics, ASCE, Vol. 5, No. 1, pp. 35–44.
11. Martin, G.R., Seed, H.B. and Finn, W.D.L (1975). "Fundamentals of Liquefaction under Cyclic Loading", Journal of the Geotechnical Engineering Division, Proceedings of ASCE, Vol. 101, No. GT5, pp. 423–438.
12. Martin, P.P. and Seed, H.B. (1979). "Simplified Procedure for Effective Stress Analysis of Ground Response", Journal of the Geotechnical Engineering Division, Proceedings of ASCE, Vol. 105, No. GT6, pp. 739–758.
13. Miwa, S., Ikeda, T. and Sato, T. (2006). "Damage Process of Pile Foundation in Liquefied Ground during Strong Ground Motion", Soil Dynamics and Earthquake Engineering, Vol. 26, No. 2–4, pp. 325–336.
14. Nath, U.K. (2006). "Pile-Soil Interaction in Liquefiable Soils", M.Tech. Thesis, Department of Civil Engineering, Indian Institute of Technology Roorkee, Roorkee.
15. Nogami, T. and Konagai, K. (1986). "Time Domain Axial Response of Dynamically Loaded Single Piles", Journal of Engineering Mechanics, ASCE, Vol. 112, No. 11, pp. 1241–1252.
16. Novak, M. (1974). "Dynamic Stiffness and Damping of Piles", Canadian Geotechnical Journal, Vol. 11, No. 4, pp. 574–598.
17. Novak, M., Nogami, T. and Aboul-Ella, F. (1978). "Dynamic Soil Reaction for Plane Strain Case", Journal of the Engineering Mechanics Division, Proceedings of ASCE, Vol. 104, No. EM4, pp. 953–959.
18. Prakash, S. (1981). "Soil Dynamics", McGraw-Hill Book Company, New York, U.S.A.
19. Seed, H.B. and Idriss, I.M. (1971). "Simplified Procedure for Evaluating Soil Liquefaction Potential", Journal of the Soil Mechanics and Foundations Division, Proceedings of ASCE, Vol. 97, No. SM9, pp. 1249–1273.
20. Seed, H.B., Martin, P.P. and Lysmer, J. (1976). "Pore-Water Pressure Changes during Soil Liquefaction", Journal of the Geotechnical Engineering Division, Proceedings of ASCE, Vol. 102, No. GT4, pp. 323–346.
21. Wilson, D.W. (1998). "Soil-Pile-Superstructure Interaction in Liquefying Sand and Soft Clay", Report UCD/CGM-98/04, Department of Civil & Environmental Engineering, University of California, Davis, U.S.A.